

## ELECTRONIC SUPPLEMENTARY INFORMATION

# Multiplexed detection of nucleic acids in a combinatorial screening chip

Benjamin R. Schudel,<sup>ac</sup> Melikhan Tanyeri,<sup>a</sup> Arnab Mukherjee,<sup>a</sup> Charles M. Schroeder,<sup>\*ab</sup>  
Paul J.A. Kenis<sup>\*ac</sup>

<sup>a</sup>Department of Chemical and Biomolecular Engineering, University of Illinois Urbana-Champaign, Urbana, Illinois 61801

<sup>b</sup>Center for Biophysics and Computational Biology, University of Illinois Urbana-Champaign, Urbana, Illinois 61801

<sup>c</sup>Center for Nanoscale Chemical Electrical Mechanical Manufacturing Systems, University of Illinois at Urbana-Champaign, Urbana, IL, USA.

### Molecular Beacon Design

The molecular beacons used in this study were developed based on successive iterations in changing sequence design and the identity of fluorophore and quencher pairs. The molecular beacons used for the final study represent the optimal sequence design within our design parameters, considering optimal surface immobilization and detection by total internal reflection microscopy. The sequences of the probe regions (corresponding to the conserved regions of four distinct viral genomes) are obtained from previous work cited in literature.<sup>1,2</sup> We specifically varied three parameters related to the stem region to optimize molecular beacon design:

- Length of the stem:** The length of the stem is critical in determining the stability and function of the molecular beacon. We used molecular beacons with 5, 6 and 8 bp stems and studied beacon stability and function both experimentally and theoretically by calculating the most energetically favorable conformation for various stem and probe sequences. Shorter stems (5 and 6 bp) generally resulted in a higher fluorescence background, likely due to destabilization of the stem upon surface immobilization. Longer stems (8 bp) generally yielded a more stable design and better quencher-fluorophore interaction, especially when the molecular beacon is immobilized on a surface.
- Location of the biotin moiety:** We characterized molecular beacons containing both internal and end-labeled biotin in the stem region and studied its effect on surface immobilization of the molecular beacon. We determined that internal biotin moieties located away from the end of the stem provided the best results in terms of surface immobilization, stem stability and molecular beacon function (quencher-fluorophore interaction).
- Fluorophore-quencher pair:** We characterized two different fluorophore-quencher pairs (Hexachlorofluorescein (HEX)/Iowa Black and Cy3/Dabcyl) and studied their effect on the signal-to-noise ratio and detection limit.

The molecular beacons listed in Table 1 in the main manuscript provided the best results in terms of stability, detection and immobilization. Table S1 lists a few of the alternative molecular beacon designs used during the process of beacon optimization in this study.

**Table S1** DNA sequences and modifications of molecular beacons used to optimize the design and functionality for this study. All sequences are shown in the 5' to 3' orientation.

---

5-bp stem, no biotin, HEX/Iowa Black fluorophore-quencher pair:

5'HEX/CCA CGC TTG TGG GTC AAC CCC CGT GG/Iowa Black/3'

6-bp stem, terminal biotin at the end of poly-A strand, internal Cy-3/Dabcyl fluorophore-quencher pair:

5'BioTEG/AAA AA/Cy3/G CTG CGT AGA GTG GTC CAA CCG CAG C/Dabcyl/3'

5-bp stem, internal biotin, HEX/Iowa Black fluorophore-quencher pair:

5'HEX/CCA CGC TTG TGG GTC AAC CCC CG/T\*/ GG/Iowa Black/3'

6-bp stem, internal biotin, HEX/Iowa Black fluorophore-quencher pair:

5'HEX/GCA GCG TAG AGT CGT CCA ACC GC/T\*/ GC/Iowa Black/3'

T\*: biotinylated nucleotide

---

## Data Analysis & Statistics

To detect for hybridized molecular beacon-target oligonucleotide complexes, fluorescence measurements were performed using TIRF microscopy within the half-wells containing the surface immobilized molecular beacons. The background signal was measured by imaging the surface-immobilized molecular beacons in each half-well prior to mixing with target oligonucleotides. Fluorescence signal was measured by imaging each half-well following the introduction and incubation of the four corresponding target oligonucleotides.

Fluorescence and background signal measurements were performed by capturing 100 successive images of three different spots (a total of 600 images) within each of the 16 half-wells. As a result, for a screening experiment with four different molecular beacons and four target oligonucleotides, we captured a total of 16 x 600 images to measure the fluorescence and background signal. An average intensity measurement for each spot (both for fluorescence and background) is obtained by calculating the mean pixel intensity value for 100 successive images. The fluorescence and background signal from each well is then obtained by determining the average and the standard deviation of the intensity measurements from three spots. The net fluorescence response upon molecular beacon-target oligonucleotide hybridization was determined by subtracting the background signal from the fluorescence signal. The uncertainty in the net fluorescence response is calculated by propagating the error from the background and fluorescence signals.

Next, we determined an average fluorescence intensity value for the molecular beacon-target oligonucleotide binding events by calculating the mean  $\pm$  standard error of the mean (SEM) of the net fluorescence response for the four positive binding events. Similarly, we calculated an average fluorescence intensity value for the negative (non-binding) events using the net fluorescence response for the twelve non-binding events. By subtracting the average intensity value for the negative (non-binding) events from the positive (binding) events, we deduced an average net fluorescence intensity value representing the detection of the binding events. The z-value is obtained by dividing this average net fluorescence intensity value by the SEM of the net fluorescence response for the twelve negative (non-binding) events. Signal-to-noise ratios (SNR) for each positive (binding) detection event are calculated by dividing the net fluorescence response by the noise. The noise is obtained by propagating the error (SEM) for the four binding (combined) and twelve unbinding (combined) events.

We report a net average fluorescence and background intensity value, and a z-value corresponding to the four molecular beacon-oligonucleotide binding/mismatch events. The rationale behind the analysis is as follows: The fluorescence and background intensity values obtained from binding/mismatch events are related to the molecular beacon sequence, including the design of the stem region (as well as the fluorophore-quencher pair and the sequence). The stem design is identical for all molecular beacons for the on-chip screening assay. Although the probe regions vary between each target oligonucleotides, the stem design and therefore majority of the beacon sequence is constant within each beacon "population".

## On-Chip Viral Nucleic Acid Marker Screening Experiment

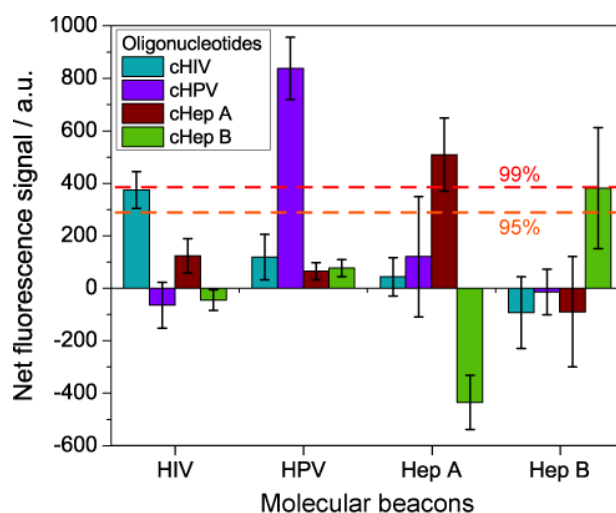


**Fig. S1** On-chip screening of oligonucleotides encoding for viral genomic content. Four molecular beacons are tested in a combinatorial fashion in their ability to detect and identify the presence of four complementary target oligonucleotides. For each molecular beacon (x-axis), only the matching target oligonucleotide showed a statistically significant positive signal. Dashed lines: upper limits of statistical confidence levels (z-test).

We repeated the on-chip viral nucleic acid marker screening experiment described in the main text. We used the 4x4 microfluidic array chip for sequence-specific detection of oligonucleotides encoding for conserved regions of the genomes of four common viruses. We immobilized four molecular beacons (100 pM) in four separate rows of the 4x4 combinatorial screening chip. Then, solutions containing the four complementary oligonucleotides (100 nM) were mixed and incubated for 1 hour with the immobilized molecular beacons to the target oligonucleotide solution.

The results of the combinatorial on-chip viral nucleic acid marker detection experiment are shown in Fig. S1. As described in the main text, the experiment was designed such that matches between molecular beacon and target oligonucleotide would be expected along the diagonal of the 4x4 array. For each molecular beacon, only the matching target oligonucleotide showed a statistically significant positive signal. The average fluorescence intensity for the four molecular beacon-oligonucleotide binding events and the twelve mismatch (non-binding) events are  $525.75 \pm 217.25$  (mean  $\pm$  standard error of the mean (SEM),  $N=4$ ) and  $-16.34 \pm 155.41$  ( $N=12$ ), respectively. A net average fluorescence intensity value of 542.08 corresponds to a z-value of 3.488 and represents the upper limit of 99.95% confidence interval. The upper limit for the 95% and 99% confidence intervals are shown in Fig. S1. The signal-to-noise ratios (SNR) for each detection event are as follows:  $\text{SNR}_{\text{HIV}}=1.46$ ,  $\text{SNR}_{\text{HPV}}=3.20$ ,  $\text{SNR}_{\text{HEP}_A}=1.97$ ,  $\text{SNR}_{\text{HEP}_B}=1.49$ . The coefficient of variation between the measurements for the four positive binding events is 0.41 suggesting a relatively small dispersion between the assays performed in the microfluidic device.

Statistical hypothesis testing is employed to discriminate between the nucleic acid detection events (molecular beacon-target oligonucleotide binding events) and the mismatch (non-binding) events. We applied the Wilcoxon Rank test to the raw experimental data for each type of viral nucleic acid marker comparing the fluorescence signal from the positive events (oligonucleotide binding/detection) with the average of the fluorescence signal from the negative (non-binding) events. The p-value obtained for the detection events was reasonably low ( $=0.0286$ ) confirming that the “hits” could not occur by mere chance.

Similar to the analysis described in the main text, we obtained larger data sets ( $N \geq 10$ ) by resampling the positive (binding) events from a normal distribution (with mean and variance equal to that of the original data set) and negative (non-binding) events by bootstrapping. The Wilcoxon Rank test is applied to each of these four larger data sets, comparing the positive and the negative events and reporting the p-value estimate for each of the four viral nucleic acid markers. The actual p-values ( $p_{\text{HIV}}=1.816 \times 10^{-4}$ ,  $p_{\text{HPV}}=1.776 \times 10^{-4}$ ,  $p_{\text{HEP}_A}=1.806 \times 10^{-4}$ ,  $p_{\text{HEP}_B}=1.688 \times 10^{-4}$ ) were significantly low, confirming the conclusions from the smaller data set.

### Statistical significance testing

Statistical significance tests provide more reliable results when the sample size increases.<sup>3</sup> In order to obtain a larger data set for the Wilcoxon test, we resampled the positive (binding) events from a normal distribution (with mean and variance equal to that of the original data set) and negative (non-binding) events by bootstrapping. For the positive (binding) events, we assumed a normal distribution to verify that the differences between the fluorescence signal from the binding and non-binding events are statistically significant in the limit of a large number of observations. Since the non-binding events could not be strictly described by a normal distribution, repeated resampling (bootstrapping) is employed to construct the synthetic larger data set for the non-binding events.

It is important to note that the Wilcoxon test is a non-parametric test, that is unlike the Student's t-test, its results are unaffected by the underlying distribution of the data sets. Nevertheless, the assumption of a normal distribution is confirmed by plotting the histograms for the fluorescence signals from the positive (binding) events (Fig. S2). The two data sets presented in the main text and supplementary information indicate a normal distribution. It is also possible to verify the normality assumption through statistical tests such as the Kolmogorov-Smirnov test.

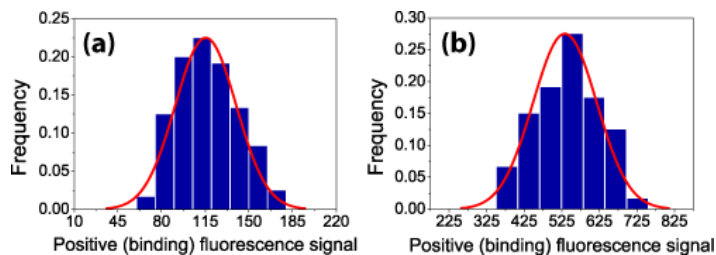


**Fig. S2** Histograms of fluorescence signal for positive (binding) events for the experimental data sets presented in the (a) main text and (b) supplementary information.

The Wilcoxon test results in a statistically significant difference (p-value  $\sim 0.03$ ) for the original experimental data sets without any resampling. The additional analysis with the larger randomly resampled data sets is employed primarily to verify that the statistically significant difference is not the result of chance alone and is indicative of a true experimental signal difference between the binding and non-binding events.

## References

1. K. Abravaya, J. Huff, R. Marshall, B. Merchant, C. Mullen, G. Schneider and J. Robinson, *Clin Chem Lab Med*, 2003, **41**, 468-474.
2. J. A. Vet, A. R. Majithia, S. A. Marras, S. Tyagi, S. Dube, B. J. Poiesz and F. R. Kramer, *Proc Natl Acad Sci U S A*, 1999, **96**, 6394-6399.
3. R. R. Sokal and F. J. Rohlf, *Biometry: the principles and practice of statistics in biological research*, W.H. Freeman, New York, 1995.